Biogeosciences
Open Access
EGU
Discussions

1 **Water availability limits tree productivity, carbon stocks, and carbon residence time in**

2 **mature forests across the western United States**

3

4 Logan T. Berner *[1], Beverly E. Law [1], and Tara W. Hudiburg [2]

5

6 [1] Department of Forest Ecosystems and Society

7 Oregon State University

8 321 Richardson Hall

9 Corvallis, Oregon 97331-2212

10

11 [2] Department of Forest, Rangeland, and Fire Sciences

12 University of Idaho

13 875 Perimeter Drive

14 Moscow, Idaho 83844-1133

15

16 * Corresponding Author:

17 logan.berner@oregonstate.edu

18 phone: 702-683-9987

19 fax: 541-737-5814

20

30

Water limits forest ecosystems in the western US

31 **Abstract**

32 Much of the western US is projected to become warmer and drier over the coming century,

33 underscoring the need to understand how climate influences terrestrial ecosystems in this region.

34 We quantified the response of tree net primary productivity (NPP), live biomass (BIO), and

35 mean carbon residence time (CRT=BIO/NPP) to spatial variation in climatic water availability in

36 the western US. We used forest inventory measurements from 1,953 mature stands (≥100 years)

37 in Washington, Oregon, and California (WAORCA) along with satellite and climate data sets

38 covering the western US. We summarized forest structure and function in both domains along a

39 400 cm yr^{-1} hydrologic gradient, quantified with a climate moisture index based on the difference

40 between precipitation and reference evapotranspiration summed from October-September (i.e.,

41 water-year) and then averaged annually from 1985-2014 ($CMI_{\overline{wy}}$). Median NPP, BIO, and CRT

42 computed at 10 cm yr^{-1} intervals along the $CMI_{\overline{wy}}$ gradient increased monotonically with

43 increasing $CMI_{\overline{wy}}$ across both WAORCA (r_s=0.93-0.96, p<0.001) and the western US (r_s=0.93-

44 0.99, p<0.001). Field measurements from WAORCA showed that median NPP increased from

45 2.2 to 5.6 Mg C ha^{-1} yr^{-1} between the driest and wettest 5% of sites, while BIO increased from 26

46 to 281 Mg C ha^{-1} and CRT increased from 11 to 49 years. The satellite data sets revealed similar

47 changes over the western US, though these data sets tended to plateau in the wettest areas,

48 suggesting that additional efforts are needed to better quantify NPP and BIO from satellites in

49 high-productivity, high-biomass forests. Our results indicate that mature forests in this region

50 were widely sensitive to changes in water availability, suggesting that projected climatic change

51 over the coming century could reduce NPP, BIO, and CRT in many parts of this region,

52 particularly the Southwest, with resulting impacts on ecosystem services.

53

1   Introduction

54

55   Climatic water availability strongly affects the distribution of plants on Earth's land surface

56   (Holdridge, 1947;Major, 1963) and the resulting structure and function of terrestrial ecosystems

57   (Schuur, 2003;Churkina and Running, 1998;Law et al., 2002). For instance, productivity of

58   desert (Whittaker and Niering, 1975), grassland (Yang et al., 2008) and forest (Schuur,

59   2003;Law et al., 2002;Berner and Law, 2015) ecosystems varies along spatial gradients in

60   climatic water availability. Climatic water availability is projected to change in many parts of the

61   world over the coming century in response to atmospheric warming from sustained

62   anthropogenic greenhouse gas emissions (Dai, 2013;Collins et al., 2013;Walsh et al., 2014).

63   Rising atmospheric temperatures increase evaporative demand (Hobbins et al., 2012) and the

64   probability that periods with anomalously low precipitation co-occur with anomalously high

65   temperatures, which increases the frequency and severity of drought (Diffenbaugh et al., 2015).

66   Societies depend on the goods and services provided by terrestrial ecosystems (e.g., forests;

67   Williams, 2006) and thus it is imperative to elucidate climatic controls over ecosystem structure

68   and function to help anticipate and mitigate potential impacts of ongoing climatic change.

69   Atmospheric warming in the western United States has increased the risk of drought and

70   continued warming over the coming century could reduce water availability in much of the

71   region (Diffenbaugh et al., 2015;Kunkel et al., 2013;Williams et al., 2012). Regional mean

72   annual temperatures increased 0.8-1.1°C from 1895 to 2011, while concomitant changes in

73   precipitation were more variable (Kunkel et al., 2013;Mote et al., 2014). Coincident with

74   regional warming there was an increase in area annually affected by drought (Cook et al., 2004)

75   and an increase in drought frequency (McCabe et al., 2004). The 2000-2004 drought was the

76   most severe drought to have occurred in the region during the past 800 years (Schwalm et al.,

77 2012). In 2013-2015, much of the western US experienced record low soil moisture and

78 mountain snowpack along with persistent high temperatures that exacerbated the multi-year

79 drought (Singh et al., 2016;Diffenbaugh et al., 2015). Climate models project mean annual

80 temperatures could further increase ~3.8-5.5°C by the end of the 21st century under a high

81 greenhouse gas emission scenario (RCP 8.5; Walsh et al., 2014;Kunkel et al., 2013). Models also

82 suggest that mean annual precipitation might increase ~10% in the northern part of the region,

83 though change little in the southern parts under the same high-emissions scenario; however,

84 these projections are more uncertain than projected changes in temperature (Walsh et al.,

85 2014;Kunkel et al., 2013). The recent severe droughts and projected increases in regional

86 atmospheric temperatures potentially foreshadow a shift towards hotter, drier conditions in much

87 of the region over the coming century (Collins et al., 2013;Dai, 2013;Williams et al.,

88 2012;Schwalm et al., 2012).

89   Changes in ecosystem structure and function along spatial climatic gradients can provide

90 insight into long-term ecosystem response to climatic change (Jin and Goulden, 2014;Biederman

91 et al., 2016;Berner et al., 2013). Mean annual precipitation varies over 500 cm yr^{-1} across the

92 western US (Daly et al., 2008) contributing to a range of ecosystems from dry desert shrublands

93 to coastal temperate rainforests (Franklin and Dyrness, 1988;Waring and Franklin, 1979) where

94 live tree biomass (BIO) attains levels thought to be exceeded only be primary *Eucalyptus*

95 *regnans* forests in southern Australia (Keith et al., 2009;Waring and Franklin, 1979). Field

96 studies carried in this region found that BIO and/or net primary productivity (NPP) tended to

97 increase as conditions became wetter (Huxman et al., 2004;Knapp and Smith, 2001;Webb et al.,

98 1983;Berner and Law, 2015;Whittaker and Niering, 1975;Gholz, 1982); however, each study

99 was based on fewer than 20 field sites selected using a set of criteria (e.g., mature forest near a

100   road). Several of these earlier studies also indicated that mean carbon residence time

101   (CRT=BIO/NPP) in live aboveground biomass (AGB) increased several fold between the driest

102   and wettest plant communities (Webb et al., 1983;Whittaker and Niering, 1975;Gholz, 1982),

103   which is potentially related to differences in disturbance regimes and carbon allocation (Girardin

104   et al., 2010). These studies illustrate that ecosystem structure and function are strongly

105   influenced by water availability in parts of the western US; however, additional efforts are

106   needed to assess forest response to variation in water availability at larger scales across this

107   region.

108   Our objective in this study was to explore how forest structure and function changed

109   along spatial gradients in climatic water availability in the western US. We hypothesized that

110   tree NPP, BIO, and CRT in mature stands (>100 years old) are constrained by water availability

111   in this region. We thus anticipated that NPP, BIO, and CRT would increase as climate became

112   wetter (or, conversely, decrease as climate became drier). We tested these hypotheses first across

113   Washington, Oregon, and California (WAORCA) using forest inventory measurements from

114   1,953 sites and then across 18 Mha of mature forest in the western US using satellite remote

115   sensing data sets that included three national biomass maps and NPP derived from the Moderate

116   Resolution Imaging Spectroradiometer (MODIS). Tree NPP, BIO, and CRT were based on

117   above- and below-ground components. We quantified water availability using a climate moisture

118   index (CMI) that accounted for the cumulative difference between precipitation (P) and reference

119   evapotranspiration (ET_0) over the approximate seasonal cycle of soil water recharge and draw-

120   down (October-September; i.e., water year).

121

122 **2   Materials and methods**

123 **2.1   Data sets and preprocessing**

124 **2.1.1   Field estimates of tree biomass, productivity, and carbon residence time**

125 We using field measurements to estimate BIO (BIO_{field}; Mg C ha^{-1}), NPP (NPP_{field}; Mg C ha^{-1} yr^{-}

126 ^{1}), and CRT (CRT_{field}; year) at 1,953 forest inventory sites located in mature stands spread across

127 WAORCA. These 1-ha sites were surveyed by the US Forest Service from 2001 to 2006 and

128 comprise a representative sample of forest lands in the region. We included sites in our analysis

129 when stand age was at least 100 years. Stand age was defined as the average age of the oldest

130 10% of trees, where individual tree age was determined on survey plots using increment cores

131 (Van Tuyl et al., 2005). BIO_{field} and NPP_{field} were computed for each site as part of a prior study

132 (Hudiburg et al., 2011). BIO_{field} was estimated using regional allometric equations for tree

133 components (e.g., stem, branch, bark, foliage, and coarse roots) based on tree diameter and/or

134 height, along with estimates of fine root mass derived from a relationship with leaf area index

135 (LAI; m^2 leaf m^{-2} ground). NPP_{field} was estimated based on changes in above- and below-ground

136 woody biomass over a 10-year interval plus annual foliage and fine root turn-over. See Hudiburg

137 et al. (2011) for additional details. *Carbon residence time* is a key ecosystem characteristic that

138 describes the average duration, in years, that a carbon molecule will remain in a specific pool

139 (e.g., live biomass; Waring and Running, 2007). We computed CRT_{field} in live tree biomass as

140 the ratio of BIO_{field} to NPP_{field} in stands averaging >100 years of age.

141

142 **2.1.2   Remote sensing estimates of tree biomass, productivity, and carbon residence time**

143   We used satellite remote sensing and ancillary data sets to estimate BIO (BIO_{sat}), NPP (NPP_{sat}),

144   and CRT (CRT_{sat}) across mature forests in the western US. BIO_{sat} included the same component

145   carbon pools as BIO_{field} (i.e, stem, branch, bark, foliage, coarse roots and fine roots). We

146   quantified the amount of carbon in stems, branches, and bark using an ensemble of three

147   satellite-derived data sets that depicted live tree aboveground biomass (AGB; excluded foliage)

148   circa 2000 to 2008 (Blackard et al., 2008;Wilson et al., 2013;Kellndorfer et al., 2012). Each map

149   was generated using satellite and geophysical (e.g., climate, topography) data sets to spatially

150   extrapolate forest inventory measurements over the conterminous US. We acquired these maps at

151   250-m spatial resolution and then converted two of the maps (Blackard et al., 2008;Kellndorfer

152   et al., 2012) from dry biomass to carbon assuming a 50% conversion factor (Smith et al., 2006).

153   We then reprojected these maps onto a uniform grid in an equal area projection, masked them to

154   the common forest extent, and then computed the ensemble average. We used the ensemble

155   average in the subsequent analysis given previous work showing that the ensemble average

156   agreed more closely with state-level estimates of tree aboveground carbon stocks derived from

157   forest inventories than any of the individual maps (Berner et al., in review).

158   After deriving spatial estimates of carbon storage in AGB, we then estimated carbon

159   storage in coarse roots, fine roots, and foliage for each 250-m forested pixel. As with AGB, we

160   assumed that roots and foliage were 50% carbon (Smith et al., 2006;Berner and Law, 2016). We

161   computed coarse root biomass based on an empirical relationship with AGB (Cairns et al., 1997)

162   and fine root biomass based on an empirical relationship with peak summer LAI (Van Tuyl et al.,

163   2005). Spatial estimates of LAI were available globally at 1-km resolution from NASA's

164   Moderate Resolution Imaging Spectroradiometer (MODIS) as part of the MOD15A2 (Collection

165   5) data set (Myneni et al., 2002). We obtained these LAI estimates at 8-day intervals during July

166   and August (late-summer) from 2000 to 2014 for the western US. We then (1) excluded poor-

167   quality pixels using the quality control flags; (2) computed average late-summer LAI over the

168   15-year period; and (3) reprojected and resampled the data set to the common 250-m resolution

169   equal area grid. We used average late-summer MODIS LAI to computed both fine root biomass

170   (as described above) and foliage biomass. Foliage biomass was estimated for each pixel by

171   dividing LAI by the average specific leaf area (SLA; g C m^{-2} leaf) of the forest type found in that

172   pixel. We aggregated an existing map of forest type (Ruefenacht et al., 2008) into nine classes

173   (e.g., *Pinus ponderosa*, true fir) and then varied SLA among classes using species-, genus-, or

174   division-specific estimates of average SLA from a recent leaf trait synthesis (Berner and Law,

175   2016). We then estimated BIO$_{sat}$ for each 250-m resolution pixel by summing the above- and

176   below-ground carbon pools.

177   We quantified regional NPP using the satellite-derived MODIS primary productivity data

178   set (NPP$_{sat}$; MOD17A3 v. 55). The MODIS light-use efficiency model predicts global terrestrial

179   NPP each year at 1-km resolution by incorporating estimates of LAI, absorbed

180   photosynthetically active radiation, and land cover derived from MODIS with plant

181   physiological characteristics and climate data (Running et al., 2004;Zhao et al., 2010). The

182   model predicts annual NPP as the cumulative difference between daily gross primary

183   productivity and daily to annual plant respiration. These estimates thus reflect NPP allocated

184   both above- and below-ground. We obtained annual NPP estimates from 2000 to 2014 for the

185   western US, reprojected the data onto an equal area grid, and then averaged over years.

186   Several additional preprocessing steps were required after deriving forest BIO$_{sat}$ and

187   NPP$_{sat}$. These included masking both BIO$_{sat}$ and NPP$_{sat}$ to areas mapped as forest by the MODIS

188   land cover map (Friedl et al., 2010) and then further masking these data sets to include only areas

189   where stand age was at least 100 years. The map of stand age reflected conditions c. 2006 and

190   was produced by Pan et al. (2011) by combining forest inventory measurements, information on

191   historical fires, and optical satellite imagery. We applied these 1-km resolution masks to the 250-

192   m resolution BIO_{sat} assuming homogenous land cover and stand age within each 1-km pixel. We

193   then average aggregated BIO_{sat} from 250-m to 1-km resolution and computed CRT_{sat} as the ratio

194   of BIO_{sat} to NPP_{sat}.

195

2.1.3   Climate date sets and derivation of the climate moisture index

197   We quantified water availability using a climate moisture index (CMI) that was computed at

198   monthly time steps as precipitation minus ET_0 (Hogg, 1994;Webb et al., 1983). We summed

199   monthly CMI over each water-year (October in year *t-1* to September in year *t*) from 1985 to

200   2014 and then averaged over years to produce a 30-year climatology ($CMI_{\overline{wy}}$; cm yr^{-1}). The

201   water year represents the approximate annual cycle of soil water recharge and withdrawal

202   (Thomas et al., 2009). We obtained estimates of monthly precipitation from the Parameter-

203   elevation Relationships on Independent Slopes Model (PRISM; Daly et al., 2008), which

204   interpolated weather station measurements onto a 4-km resolution grid. We then estimated

205   monthly ET_0 using the Food and Agricultural Organizations (FAO) Penman-Monteith equation

206   (FAO-56; Allen et al., 1998), where

207
$$ET_0 = \frac{0.408\Delta\left(R_n - G\right) + \gamma\left(\frac{900}{T + 273}\right)U(e_s - e_a)}{\Delta + \gamma\left(1 + 0.34\,U\right)}$$

208   Variables included net incoming radiation (R_n), soil heat flux (G), mean daily temperature (T),

209   wind speed (U), and both saturation (e_s) and actual vapor pressure (e_a), as well as the

210   psychrometric constant (γ) and the slope of the vapor pressure curve (Δ). We quantified R_n and U

211   using monthly climatologies from the North American Land Data Assimilation System-2

212   (NALDAS-2) that were based on measurements from 1980-2009 (Mitchell et al., 2004). We

213   derived G, T, e_s, and e_a from PRISM temperature data following Zotarelli et al. (2010). After

214   computing $\mathrm{CMI}_{\overline{wy}}$, we then resampled these data using the nearest neighbor approach to match

215   the footprints of both the 1-km NPP and 250-m BIO remote sensing data sets.

216

2.2   Analysis

218   We quantified the response of forest NPP, BIO, and CRT to changes in $\mathrm{CMI}_{\overline{wy}}$ across both

219   WAORCA and the broader western US. We specifically focused on areas where $\mathrm{CMI}_{\overline{wy}}$ was

220   between -200 and 200 cm yr^{-1}, conditions which occurred both in WAORCA and in the broader

221   region. This range encompassed 98% of forest area in the western US; the paucity of data in the

222   remaining 2% of forest area that was either drier or wetter precluded rigorous analysis. We

223   divided the landscape along this gradient into 10 cm yr^{-1} non-overlapping bins and then

224   summarized forest characteristics in each bin by computing the median, along with the 10th, 25th,

225   75th and 90th percentiles. Forest characteristics were summarized separately for the field and

226   remote sensing data sets. There were a minimum of 10 and a maximum of 114 field sites in each

227   bin. We then assessed the association between the median forest characteristic (i.e., NPP, BIO,

228   and CRT) in each bin and $\mathrm{CMI}_{\overline{wy}}$ across the ecoclimatic gradient using nonparametric

229   Spearman's rank correlation. This test yields a coefficient (r_s) between -1 and +1, where a value

230   of +1 indicates a perfect monotonically increasing relationship, a value of zero indicates no

231   covariation between the two variables, and a value of -1 indicates a perfect monotonically

232   decreasing relationship. The test is analogous to Pearson's correlation where the data have first

233   been ranked. We assessed the association between forest characteristics and $CMI_{\overline{wy}}$ using

234   Spearman's correlation rather than nonlinear regression because our intent was to describe the

235   general relationship rather than develop a predictive model. We performed data preprocessing,

236   analysis, and visualization using ArcGIS 10 (ESRI, Redlands, CA) and *R* statistical software (R

237   Core Team, 2015), relying extensive on the *R* packages *raster* (Hijmans and van Etten, 2013)

238   and *dplyr* (Wickham and Francois, 2015).

239

2.3   Uncertainty

241   We minimize uncertainty in our analysis by incorporating satellite and field data sets, as well as

242   by examining the sensitivity of $CMI_{\overline{wy}}$ to methods used to estimate ET_0. Specifically, we

243   characterized forest BIO using three satellite-derived maps and field inventories. We similarly

244   characterized forest NPP using both satellite and field inventory data sets. This approach

245   combines the strengths of spatially continuous satellite-based model output with the rigor of

246   spatially-limited, field-based inventory measurements. Additionally, we computed $CMI_{\overline{wy}}$ based

247   on ET_0 derived using both the FAO-56 (Allen et al., 1998) and modified-Hargreaves (Hargreaves

248   and Samani, 1985;Droogers and Allen, 2002) methods. This comparison revealed that our results

249   were robust to differences in methods (results not shown) and thus we focused on $CMI_{\overline{wy}}$

250   computed using the FAO-56 method.

251

3   Results

252

253   Average annual climatic water availability varied widely across both WAORCA and the broader

254   western US from 1985-2014 (Fig. 1a, b). The $CMI_{\overline{wy}}$ ranged from around -400 cm yr^{-1} in

255   southern California and Arizona to over 400 cm yr^{-1} in the coastal mountain ranges in

256   northwestern Washington and Oregon. Forests mapped by MODIS occurred in areas where

257    $CMI_{\overline{wy}}$ was between -340 and 490 cm yr^{-1}, though 98% of forest area occurred between -200 and

258   200 cm y^{-1}, and 72% occurred between -100 and 100 cm yr^{-1}. Average (±1 SD) $CMI_{\overline{wy}}$ in

259   forested areas was -40±80 cm yr^{-1}. The Coast Range and Cascade Mountains in Washington and

260   Oregon were the wettest areas, with $CMI_{\overline{wy}}$ generally >100 cm yr^{-1}. Water availability decreased

261   rapidly in the rain shadows east of the Cascades and Sierra Nevada, giving rise to very steep

262    $CMI_{\overline{wy}}$ gradients. For instance, annual $CMI_{\overline{wy}}$ in northern Oregon decreased nearly 350 cm over

263   ~30 km between high-elevation forests in the Cascades and low-elevation woodlands in the

264   eastern foothills of the Cascades. The range in $CMI_{\overline{wy}}$ encountered along this gradient in the

265   Cascades almost spanned the full range in $CMI_{\overline{wy}}$ that supported 98% of forest area in the

266   western US. Dry forests occurred along the low-elevation margins of mountain ranges

267   throughout continental areas, though the largest tract of dry forest was found in Arizona and New

268   Mexico.

269   Forest NPP, BIO, and BIO residence time varied substantially across both WAORCA and

270   the broader western US in response to variation in $CMI_{\overline{wy}}$ (Fig. 1, 2, Table 2). We focused on

271   forests in areas where $CMI_{\overline{wy}}$ was between -200 and 200 cm yr^{-1} given the paucity of land and

272   measurements in the 2% of forest area that was either drier or wetter. Median NPP_{field}, BIO_{field},

273   and CRT_{field} all exhibited a strong, positive association with $CMI_{\overline{wy}}$ (r_s=0.93-0.96, p<0.001).

274   Median NPP_{field} increased 155% between the driest and wettest 5% of sites in WAORCA (Fig.

275   2a), while median BIO_{field} and CRT_{field} increased 997% and 358%, respectively, between these

276   sites (Fig. 2b, c; Table 2). The relationship in each case was slightly curvilinear. There were also

277   strong, positive relationships among median NPP_{field}, BIO_{field}, and CRT_{field} along the WAORCA

278   ecoclimatic gradient (r_s=0.90-0.96, p<0.001).

279   Broadly similar patterns were evident when forest NPP_{sat}, BIO_{sat}, and CRT_{sat} were

280   examined across the western US using remote sensing data sets (Fig. 1b, c, d, 2c, d; Table 2).

281   Median NPP_{sat}, BIO_{sat}, and CRT_{sat} all showed a strong, positive relationship with $CMI_{\overline{wy}}$

282   (r_s=0.93-0.99; p<0.001). Median NPP_{sat} increased 97% between the driest and wettest 5% of

283   forested areas along the regional $CMI_{\overline{wy}}$ gradient (Fig. 2d, Table 2). Similarly, median BIO_{sat} and

284   CRT_{sat} increased 410% and 160%, respectively, between the driest and wettest areas (Fig. 2e, f,

285   Table 2). The response of median NPP_{sat}, BIO_{sat}, and CRT_{sat} to increased $CMI_{\overline{wy}}$ was more

286   curvilinear than the responses observed in the field measurements, with the satellite data sets

287   plateauing in areas where annual $CMI_{\overline{wy}}$ was above ~100 cm. Furthermore, while magnitude of

288   NPP_{sat} and NPP_{field} response to $CMI_{\overline{wy}}$ were similar, the magnitude of BIO_{sat} and CRT_{sat}

289   responses to increased $CMI_{\overline{wy}}$ were much more muted than the magnitude of response in BIO_{field}

290   and CRT_{field}. There were again strong relationships among median NPP_{sat}, BIO_{sat}, and CRT_{sat}

291   along the western US ecoclimatic gradient (r_s=0.93-0.97, p<0.001).

292

293   **4**   **Discussion and conclusions**

294   **4.1**   **Climate moisture index**

295   Climatic water availability exerted a strong influence on NPP, BIO, and CRT among mature

296   forests in the western US. We chose to quantify climatic water availability using an index that

297   accounted for both precipitation and energy-mediated ET_0, recognizing that both of these factors

298   contribute to the relative water stress experienced by plants within an ecosystem (Webb et al.,

299   1983). We acknowledge that this index has several short-comings. For instance, the index does

300   not account for spatial variation in soil water storage capacity, which can be crucial for

301   determining plant performance during drought (Peterman et al., 2013). This might explain some

302   of the variation in NPP and BIO among areas with similar $CMI_{\overline{wy}}$; however, quantifying soil

303   water storage capacity even at individual sites is challenging given uncertainty in soil structure

304   and plant rooting capacity (Running, 1994). The index also does not account for water added via

305   fog drip, which has been shown to supply 13-45% of the water transpired by redwood forests (*S.*

306   *sempervirens*) (Dawson, 1998) and sustain other forest ecosystems along the California coast

307   (Fischer et al., 2016;Johnstone and Dawson, 2010). This potentially explains why there were

308   areas with low $CMI_{\overline{wy}}$ along the central and northern coast of California that supported forests

309   with higher NPP and BIO than other forests with similar $CMI_{\overline{wy}}$. Furthermore, the index does not

310   account for spatial variation in runoff and thus likely overestimates water availability in the

311   wettest areas since the fraction of water lost as run-off increases with precipitation (Sanford and

312   Selnick, 2013). Despite its relative simplicity, prior studies showed that CMI was a useful index

313   for explaining interannual variability in fire activity in the southwest US (Williams et al., 2014),

314   as well as forest productivity in northern Siberia (Berner et al., 2013), southern Canada (Hogg et

315   al., 2002), and central Oregon (Berner and Law, 2015). Several studies also found that the index,

316   or its inverse (i.e. ET_0 - P), explained substantial spatial variability in mature forest gross

317   photosynthesis (Law et al., 2002), productivity and biomass across a range of ecosystems

318 (Berner and Law, 2015;Webb et al., 1983;Hogg et al., 2008). Our current study further

319 demonstrates that CMI is a useful, empirical index for assessing climatic constraints on forest

320 ecosystems at large spatial scales.

321

4.2   Tree net primary productivity

323 Median forest NPP in mature stands approximately doubled between the driest and wettest areas

324 in both WAORCA and the western US, though in both cases the rate at which NPP increased

325 with $CMI_{\overline{wy}}$ slowed in the wettest areas. Prior field studies conducted at a limited number of field

326 sites in the western US over the past four decades have similarly documented increased forest

327 NPP along spatial gradients of increasing water availability (Webb et al., 1983;Whittaker and

328 Niering, 1975;Gholz, 1982;Berner and Law, 2015). Our current study demonstrates a robust

329 relationship between mature forest NPP and climatic water availability using field measurements

330 from nearly 2,000 inventory plots along with satellite remote sensing data sets covering ~18

331 Mha. The NPP-$CMI_{\overline{wy}}$ relationship was similar when NPP was assessed using field

332 measurements from across WAORCA or using MODIS covering the western US, though

333 MODIS showed NPP leveling off in the wettest areas ($CMI_{\overline{wy}} \approx$ 100-200 cm yr^{-1}), whereas this

334 was less evident in the field measurements. A recent remote sensing analysis of California used

335 absorbed photosynthetically-active radiation (APAR) derived from MODIS as an index of gross

336 primary productivity and found that APAR increased asymptotically with increasing mean

337 annual precipitation across vegetation communities (Jin and Goulden, 2014). Forests—

338 occupying the wettest areas and having the highest APAR—exhibited the smallest increase in

339 APAR per unit increase in precipitation of any vegetation community whether assessed along a

340   spatial or a temporal gradient, suggesting that forests were less sensitive to changes in

341   precipitation than other vegetation communities (Jin and Goulden, 2014). The lack of asymptotic

342   response in our field measurements together with the asymptotic response of both MODIS NPP

343   and APAR suggests that climate impact assessments based on MODIS could underestimate the

344   sensitivity of NPP to changes in water availability in wet, densely forested area.

345   Mechanistically, the strong NPP-CMI$_{\overline{wy}}$ association reflects the coupling between carbon

346   and water cycling at leaf (Ball et al., 1987) to ecosystem scales (Law et al., 2002). Forest NPP

347   depends on regionally-specific relations with leaf area (Waring, 1983;Schroeder et al., 1982),

348   which largely determine the proportion of incoming solar radiation that is absorbed and thus

349   potentially available to fuel photosynthesis (Runyon et al., 1994). Leaf photosynthesis inevitably

350   leads to transpiration water loss (Ball et al., 1987) that must be balanced against water uptake

351   from the soil so as to prevent the formation of excessive tension on the internal water column

352   that could result in hydraulic failure (Ruehr et al., 2014;Williams et al., 1996). As soil water

353   availability increases, trees are able to support greater leaf area while maintaining water column

354   tensions within physiologically operable ranges, which consequently leads to more

355   photosynthate available to fuel NPP unless trees are limited by other resources (e.g., nitrogen).

356   The decreasing rate at which NPP increased with CMI$_{\overline{wy}}$ in the wettest areas is likely due to low

357   temperatures constraining productivity at high-elevations (Nakawatase and Peterson,

358   2006;Runyon et al., 1994) and heavy cloud-cover limiting solar radiation and thus

359   photosynthesis in coastal areas (Carroll et al., 2014;Zhao et al., 2010). Forest NPP is affected by

360   many biotic (e.g., age) and abiotic factors (e.g., nutrients), yet climatic water availability emerges

361   as a key environmental constraint in the western US.

362

4.3   Tree carbon stocks

364   Mature forest BIO increased notably with increasing $CMI_{\overline{wy}}$ across both WAORCA and the

365   broader western US, reflecting underlying shifts in NPP and, likely, tree mortality due to

366   disturbance. BIO is determined by the rates at which carbon is gained via NPP and lost due to

367   tissue senescence and mortality integrated over annual to centennial time scales (Olson, 1963).

368   Hence, the increase in NPP with increasing $CMI_{\overline{wy}}$ explains some of the concomitant increase in

369   BIO. We suspect that as conditions became wetter there was also a decline in the proportion of

370   BIO lost to annual mortality from natural disturbances. Several recent studies found that tree

371   mortality rates due to bark beetles and fires were very low in the wettest parts of the western US

372   (e.g., Coast Range and Cascades), while considerably higher in most drier areas (Berner et al., in

373   review;Hicke et al., 2013). Furthermore, the field and satellite data sets also incidentally revealed

374   there was an increase in the median age of stands over 100 years as conditions became wetter,

375   with median stand age ~140 years in the driest areas and 200-240 years in the wettest areas. The

376   general increase in mature forest BIO with increasing water availability is thus likely due to

377   higher rates of productivity and lower rates of mortality from natural disturbance.

378   The observed increase in mature forest BIO with increasing climatic water availability

379   was generally consistent with prior field studies from this region, yet our study demonstrates this

380   response over a much broader ecoclimatic gradient. For instance, early work by Whittaker and

381   Niering (1975) showed that mature forest BIO tended to increase with a moisture index inferred

382   from community composition along an elevational gradient in Arizona's Santa Catalina

383   Mountains. Subsequent studies focused on five LTER sites spread across the conterminous US

384   (Webb et al., 1983) and at sites in Oregon (Berner and Law, 2015;Gholz, 1982) similarly showed

385   a general increase in tree biomass with increasing water availability. Our study included sites

386   that ranged from dry woodlands with little BIO to temperate rainforests with BIO exceeded in

387   few other regions (e.g. max BIO ≈ 950 Mg C ha^{-1}). BIO in our study area has been reported to

388   reach over 2,000 Mg C ha^{-1} in old-growth coastal redwood stands in northern California (Waring

389   and Franklin, 1979), which is thought to be exceeded only by the >3,000 Mg C ha^{-1} attained by

390   old-growth *Eucalyptus regnans* stands in southern Australia (Keith et al., 2009). A global

391   synthesis suggested that average AGB among high-biomass stands in wet temperate forests

392   (~377 Mg C ha^{-1}) was over twice that of high-biomass stands in wet tropical forests (~179 Mg C

393   ha^{-1}) and nearly six times that of high-biomass stands in wet boreal forests (~64 Mg C ha^{-1})

394   (Keith et al., 2009). The range in mature forest BIO included in our analysis of WAORCA thus

395   spanned much of the observed global range in BIO.

396   Both field and satellite measurements revealed that median BIO increased with $CMI_{\overline{wy}}$,

397   yet the satellite data set showed less of an increase than the field measurements. Median forest

398   BIO_{field} increased nearly 1,000% between the dry woodlands and coastal temperate rainforests in

399   WAORCA, yet the increase in BIO_{sat} with increasing $CMI_{\overline{wy}}$ was less pronounced (410%

400   increase) when assessed across the western US. Furthermore, median BIO_{sat} plateaued around

401   175 Mg C ha^{-1} in areas where $CMI_{\overline{wy}}$ was ~100-200 cm yr^{-1}. The response of BIO to increasing

402    $CMI_{\overline{wy}}$ was likely more muted when assessed using the satellite-derived maps than the field

403   measurements for several reasons. Areas with high BIO often occur as small patches set in a

404   matrix of stands with lower BIO (Spies et al., 1994) and thus the moderate-resolution satellite

405   imagery used in developing these maps records the spectral signature of this larger area rather

406   than just the patch with high BIO. In other words, the satellite imagery has a larger sampling

407 footprint relative to that of a field plot, which thus averages BIO over a larger area, reducing

408 peak values. Additionally, the maps are largely derived from optical, multi-spectral satellite

409 imagery that is not very sensitive to variation in BIO in high-biomass forests. Advances in

410 satellite remote sensing, such as NASA's new Global Ecosystem Dynamics Investigation Lidar

411 (GEDI) instrument, are anticipated to help overcome some of these challenges (Goetz and

412 Dubayah, 2011). Nevertheless, current BIO maps (e.g., Wilson et al., 2013;Kellndorfer et al.,

413 2012) proved a valuable tool for ecologic and natural resource assessments (Goetz et al.,

414 2014;Krankina et al., 2014;Berner et al., in review).

415

416 **4.4   Carbon residence time in tree biomass**

417 Median CRT_{field} increased persistently with $\overline{CMI_{wy}}$ from ~11 years in the driest forests to over 49

418 years in the wettest forests, highlighting a fundamental change in ecosystem function along this

419 broad ecoclimatic gradient. A prior study focused on 11 LTERS spread across the conterminous

420 US found that CRT increased from ~2 years in a desert shrubland to ~73 years in 450-years old

421 Douglas-fir stand at the Andrews LTER in the Oregon Cascade Mountains (Webb et al., 1983).

422 For comparison, we looked at five old-growth Douglas-fir stands (336-555 years old) near the

423 Andrews LTER and found that CRT averaged 79±23 years (± 1SD) among these stands. An

424 increase in the CRT of aboveground tissues was also observed among plant communities along

425 an elevational moisture gradient in the Arizona Santa Catalina Mountains (Whittaker and

426 Niering, 1975) and across nine mature stands in a range of forest types in Oregon (Gholz, 1982).

427 Although this pattern has been documented in several instances, the underlying mechanisms

428 remain unclear.

429   We speculate that the increase in CRT with increased water availability was potentially

430   associated with underlying changes in NPP allocation and BIO mortality rates. Trees invest a

431   larger proportion of NPP into aboveground tissue production as conditions become wetter and

432   competition for light intensifies (Runyon et al., 1994;Law et al., 2003). Our field measurements

433   revealed that the fraction of NPP allocated aboveground increased from ~0.45 in the driest areas

434   to ~0.64 in the wettest areas and, furthermore, that CRT in aboveground tissues averaged twice

435   as long as the CRT in belowground tissues. Thus, a shift in NPP allocation toward longer-lived

436   aboveground tissues likely contributed to the observed increase in CRT as conditions become

437   wetter, as might changes in BIO mortality rates along this hydraulic gradient. Recent BIO

438   mortality rates due to disturbance by wildfires and bark beetles tended to be considerably lower

439   in the wettest parts of the western US than in drier parts of the region (Berner et al., in review).

440   The incidental observation that mature stands tended to be older in the wetter areas is consistent

441   with these areas experiencing lower morality rates from natural disturbances. Our study

442   demonstrates that CRT in live tree biomass was strongly influenced by water availability, yet

443   additional efforts are needed to elucidate underlying mechanism affecting CRT, particularly

444   given that CRT is a primary source of uncertainty in global vegetation model projections of

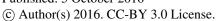445   future terrestrial carbon cycling (Friend et al., 2014).

446

447   **4.5   Climate change implications**

448   Forest NPP, BIO, and CRT in mature stands increased with $CMI_{\overline{wy}}$ across WAORCA and the

449   broader western US, underscoring that climatic water availability is a major abiotic constraint on

450   several keys aspects of ecosystem structure and function in forests ranging from dry woodlands

451   to coastal temperate rainforests. What do these findings mean in the context of regional climate

452   change? Although future changes in precipitation are uncertain, climate models widely project

453   extensive regional warming over the coming century in response to high rates of greenhouse gas

454   emissions, which could lead to drier conditions as higher temperatures increase atmospheric

455   evaporation demand (Walsh et al., 2014;Collins et al., 2013;Dai, 2013). For instance, simulations

456   based on the sophisticated Variable Infiltration Capacity (VIC) hydraulic model and a high-

457   emission scenario (A2) suggest that soil moisture could decline ~1-15% in many parts of the

458   region by the end of the 21st century, with drying particularly acute in the Southwest (Walsh et

459   al., 2014). Similarly, a large ensemble of climate models indicate that soil moisture could decline

460   3-12% throughout the region over this century (Dai, 2013). In fact, projections of regional drying

461   are widespread, particularly for the Southwest (e.g., Williams et al., 2012;Schwalm et al.,

462   2012;Burke et al., 2006;Seager and Vecchi, 2010;Dai, 2011;Collins et al., 2013).

463   Increased atmospheric CO_2 and warming in the Northwest could enhance tree

464   productivity in some areas by (1) increasing water use efficiency (WUE) through CO_2

465   fertilization and (2) enhancing spring photosynthesis (Ruehr et al., 2014;Hudiburg et al.,

466   2013;Kang et al., 2014;Soulé and Knapp, 2015). On the other hand, many tree species have

467   narrow hydraulic safety margins (Choat et al., 2012) and warming-induced declines in tree

468   growth have occurred in other regions despite increased WUE (Andreu-Hayles et al.,

469   2011;Peñuelas et al., 2011;Lévesque et al., 2014). It is unlikely that increased WUE and other

470   physiological adjustments will fully compensate for impacts of rapid future warming on tree

471   physiology (Allen et al., 2015), especially in the Southwest where hotter and drier conditions are

472   already suppressing tree productivity and increasing tree mortality in some areas (Dennison et

473   al., 2014;Creeden et al., 2014;Williams et al., 2012;Anderegg et al., 2015;McDowell et al.,

474   2015). The strong NPP-CMI$_{\overline{wy}}$, BIO-CMI$_{\overline{wy}}$, and CRT-CMI$_{\overline{wy}}$ associations that we observed in

475   the western US suggest that future reductions in water availability will likely reduce NPP, BIO,

476   and CRT in mature forests, particularly those in the driest areas.

477

478   **4.6   Conclusions**

479   Forests in the western US range from dry woodlands to temperate rainforests, an ecological

480   gradient that nearly spans the global range in tree biomass and that largely reflects spatial

481   variation in climatic water availability. In this study, we quantified changes in tree productivity,

482   live biomass, and carbon residence time along spatial gradients in climatic water availability

483   using field inventory measurements from WAORCA and satellite remote sensing data sets

484   spanning the western US. Our multi-method, multi-scale analysis revealed that tree productivity,

485   live biomass, and carbon residence time all increased notably with climatic water availability,

486   which was computed using an index that accounted for both precipitation and reference

487   evapotranspiration. The observed increase in productivity was likely due to the close coupling

488   between carbon and water cycling at leaf to ecosystem scales, while the observed increase in live

489   biomass was likely due to the increased productivity and stand age, along with a decreased

490   proportion of live biomass lost to annual mortality. Forest productivity and biomass derived from

491   field- and satellite-measurements exhibited broadly similar sensitivities to changes in climatic

492   water availability, though the satellite data sets tended to plateau in the wettest areas, suggesting

493   that additional efforts are needed to better quantify productivity and biomass from satellites in

494   high-productivity, high-biomass forests. The pronounced increase in carbon residence time with

495   increasing water availability suggests that efforts to increase terrestrial carbon storage as a tool to

496   combat climate change will be most effective in the wettest areas. Furthermore, the observed

497   change in carbon residence time could provide a benchmark for evaluating the performance of

498   global vegetation models, in which carbon residence time is a principle source of uncertainty in

499   future projections of the global carbon cycle. Overall, our results indicate that tree productivity,

500   live biomass, and carbon residence time in mature stands are widely sensitive to changes in

501   climatic water availability in the western US, suggesting that projected warming and drying over

502   the coming century due to business-as-usual greenhouse gas emissions could have important

503   impacts on ecosystem structure, function, and services in many parts of this region.

504

Author contributions

506   L.T.B. designed the study, analyzed the data, and prepared the manuscript with contributions

507   from B.E.L. and T.W.H., who both also contributed data sets to this effort.

508

516

References

518 Allen, C. D., Breshears, D. D., and McDowell, N. G.: On underestimation of global vulnerability to tree

519 mortality and forest die-off from hotter drought in the Anthropocene, Ecosphere, 6, 1-55, 2015.

520 Allen, R. G., Pereira, L. S., Raes, D., and Smith, M.: Crop evapotranspiration-Guidelines for computing

521 crop water requirements-FAO Irrigation and drainage paper 56, FAO, Rome, 300, 1998.

522 Anderegg, W. R., Flint, A., Huang, C.-y., Flint, L., Berry, J. A., Davis, F. W., Sperry, J. S., and Field, C. B.:

523 Tree mortality predicted from drought-induced vascular damage, Nature Geoscience, 8, 367-371,

524 10.1038/ngeo2400, 2015.

525 Andreu-Hayles, L., Planells, O., Gutierrez, E., Muntan, E., Helle, G., Anchukaitis, K. J., and Schleser, G. H.:

526 Long tree-ring chronologies reveal 20th century increases in water-use efficiency but no enhancement

527 of tree growth at five Iberian pine forests, Global Change Biology, 17, 2095-2112, 2011.

528 Ball, J. T., Woodrow, I. E., and Berry, J. A.: A model predicting stomatal conductance and its contribution

529 to the control of photosynthesis under different environmental conditions, in: Progress in

530 photosynthesis research, Springer, 221-224, 1987.

531 Berner, L. T., Beck, P. S. A., Bunn, A. G., and Goetz, S. J.: Plant response to climate change along the

532 forest-tundra ecotone in northeastern Siberia, Global Change Biology, 19, 3449-3462,

533 10.1111/gcb.12304, 2013.

534 Berner, L. T., and Law, B. E.: Water limitations on forest carbon cycling and conifer traits along a steep

535 climatic gradient in the Cascade Mountains, Oregon, Biogeosciences, 12, 6617-6635, 2015.

536 Berner, L. T., and Law, B. E.: Plant traits, productivity, biomass and soil properties from forest sites in the
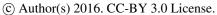
537 Pacific Northwest, 1999–2014, Scientific Data, 3, 160002, 10.1038/sdata.2016.2, 2016.

538   Berner, L. T., Law, B. E., Meddens, A. J. H., and Hicke, J. A.: Regional assessment of forest biomass,

539   productivity, and mortality from disturbance across the western US (2003-2012), in review.

540   Biederman, J., Scott, R., Goulden, M., Vargas, R., Litvak, M., Kolb, T., Yepez, E., Oechel, W., Blanken, P.,

541   and Bell, T.: Terrestrial carbon balance in a drier world: the effects of water availability in southwestern

542   North America, Global change biology, 2016.

543   Blackard, J., Finco, M., Helmer, E., Holden, G., Hoppus, M., Jacobs, D., Lister, A., Moisen, G., Nelson, M.,

544   and Riemann, R.: Mapping US forest biomass using nationwide forest inventory data and moderate

545   resolution information, Remote Sensing of Environment, 112, 1658-1677, 2008.

546   Burke, E. J., Brown, S. J., and Christidis, N.: Modeling the recent evolution of global drought and

547   projections for the twenty-first century with the Hadley Centre climate model, Journal of

548   Hydrometeorology, 7, 2006.

549   Cairns, M. A., Brown, S., Helmer, E. H., and Baumgardner, G. A.: Root biomass allocation in the world's

550   upland forests, Oecologia, 111, 1-11, 1997.

551   Carroll, A. L., Sillett, S. C., and Kramer, R. D.: Millennium-Scale Crossdating and Inter-Annual Climate

552   Sensitivities of Standing California Redwoods, PLoS ONE, 9, e102545, 10.1371/journal.pone.0102545,

553   2014.

554   Choat, B., Jansen, S., Brodribb, T. J., Cochard, H., Delzon, S., Bhaskar, R., Bucci, S. J., Feild, T. S., Gleason,

555   S. M., Hacke, U. G., Jacobsen, A. L., Lens, F., Maherali, H., Martinez-Vilalta, J., Mayr, S., Mencuccini, M.,

556   Mitchell, P. J., Nardini, A., Pittermann, J., Pratt, R. B., Sperry, J. S., Westoby, M., Wright, I. J., and Zanne,

557   A. E.: Global convergence in the vulnerability of forests to drought, Nature, 491, 752-755,

558   doi:10.1038/nature11688, 2012.

559   Churkina, G., and Running, S. W.: Contrasting climatic controls on the estimated productivity of global

560   terrestrial biomes, Ecosystems, 1, 206-215, 1998.

561   Collins, M., Knutti, R., Arblaster, J., Dufresne, J.-L., Fichefet, T., Friedlingstein, P., Gao, X., Gutowski, W. J.,

562   Johns, T., Krinner, G., Shongwe, M., Tebaldi, C., Weaver, A. J., and Wehner, M.: Long-term Climate

563   Change: Projections, Commitments and Irreversibility, in: Climate Change 2013: The Physical Science

564   Basis. Contribution of Working Group I to the Fifth Assessment Report of the Intergovernmental Panel

565   on Climate Change, edited by: Stocker, T. F., Qin, D., Plattner, G.-K., Tignor, M., Allen, S. K., Boschung, J.,

566   Nauels, A., Xia, Y., Bex, V., and Midgley, P. M., Cambridge University Press, Cambridge, United Kingdom

567   and New York, NY, USA, 1029–1136, 2013.

568   Cook, E. R., Woodhouse, C. A., Eakin, C. M., Meko, D. M., and Stahle, D. W.: Long-term aridity changes in

569   the western United States, Science, 306, 1015-1018, 2004.

570   Creeden, E. P., Hicke, J. A., and Buotte, P. C.: Climate, weather, and recent mountain pine beetle

571   outbreaks in the western United States, Forest Ecology and Management, 312, 239-251,

572   http://dx.doi.org/10.1016/j.foreco.2013.09.051, 2014.

573   Dai, A.: Drought under global warming: a review, Wiley Interdisciplinary Reviews: Climate Change, 2, 45-

574   65, 2011.

575   Dai, A.: Increasing drought under global warming in observations and models, Nature Climate Change, 3,

576   52-58, doi: 10.1038/nclimate1633, 2013.

577   Daly, C., Halbleib, M., Smith, J. I., Gibson, W. P., Doggett, M. K., Taylor, G. H., Curtis, J., and Pasteris, P. P.:

578   Physiographically sensitive mapping of climatological temperature and precipitation across the

579   conterminous United States, International Journal of Climatology, 28, 2031-2064, 2008.

580   Dawson, T. E.: Fog in the California redwood forest: ecosystem inputs and use by plants, Oecologia, 117,

581   476-485, 1998.

582   Dennison, P. E., Brewer, S. C., Arnold, J. D., and Moritz, M. A.: Large wildfire trends in the western United

583   States, 1984–2011, Geophysical Research Letters, 41, 2014GL059576, 10.1002/2014GL059576, 2014.

584 Diffenbaugh, N. S., Swain, D. L., and Touma, D.: Anthropogenic warming has increased drought risk in

585 California, Proceedings of the National Academy of Sciences, 112, 3931-3936, 2015.

586 Droogers, P., and Allen, R. G.: Estimating reference evapotranspiration under inaccurate data conditions,

587 Irrigation and drainage systems, 16, 33-45, 2002.

588 Fischer, D. T., Still, C. J., Ebert, C. M., Baguskas, S. A., and Park Williams, A.: Fog drip maintains dry

589 season ecological function in a California coastal pine forest, Ecosphere, 7, 2016.

590 Franklin, J. F., and Dyrness, C. T.: Natural vegetation of Oregon and Washington, in, Oregon State

591 University Press, Corvallis, 452, 1988.

592 Friedl, M. A., Sulla-Menashe, D., Tan, B., Schneider, A., Ramankutty, N., Sibley, A., and Huang, X.: MODIS

593 Collection 5 global land cover: Algorithm refinements and characterization of new datasets, Remote

594 Sensing of Environment, 114, 168-182, 2010.

595 Friend, A. D., Lucht, W., Rademacher, T. T., Keribin, R., Betts, R., Cadule, P., Ciais, P., Clark, D. B.,

596 Dankers, R., and Falloon, P. D.: Carbon residence time dominates uncertainty in terrestrial vegetation

597 responses to future climate and atmospheric CO2, Proceedings of the National Academy of Sciences,

598 111, 3280-3285, 2014.

599 Gholz, H. L.: Environmental Limits on Aboveground Net Primary Production, Leaf Area, and Biomass in

600 Vegetation Zones of the Pacific Northwest, Ecology, 63, 469-481, 10.2307/1938964, 1982.

601 Girardin, C. A. J., Malhi, Y., Aragao, L., Mamani, M., Huaraca Huasco, W., Durand, L., Feeley, K., Rapp, J.,

602 SILVA-ESPEJO, J., and Silman, M.: Net primary productivity allocation and cycling of carbon along a

603 tropical forest elevational transect in the Peruvian Andes, Global Change Biology, 16, 3176-3192, 2010.

604 Goetz, S., and Dubayah, R.: Advances in remote sensing technology and implications for measuring and

605 monitoring forest carbon stocks and change, Carbon Management, 2, 231-244, 10.4155/cmt.11.18,
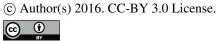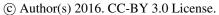
606 2011.

607   Goetz, S. J., Sun, M., Zolkos, S., Hansen, A., and Dubayah, R.: The relative importance of climate and

608   vegetation properties on patterns of North American breeding bird species richness, Environmental

609   Research Letters, 9, 034013, 2014.

610   Hargreaves, G. H., and Samani, Z. A.: Reference crop evapotranspiration from temperature, Applied

611   Engineering in Agriculture, 1, 96-99, 1985.

612   Hicke, J. A., Meddens, A. J., Allen, C. D., and Kolden, C. A.: Carbon stocks of trees killed by bark beetles

613   and wildfire in the western United States, Environmental Research Letters, 8, 035032, 2013.

614   Hijmans, R. J., and van Etten, J.: raster: Geographic analysis and modeling with raster data, 2.1-25 ed., R

615   Foundation for Statistical Computing, Vienna, 2013.

616   Hobbins, M., Wood, A., Streubel, D., and Werner, K.: What drives the variability of evaporative demand

617   across the conterminous United States?, Journal of Hydrometeorology, 13, 1195-1214, 2012.

618   Hogg, E., Brandt, J. P., and Kochtubajda, B.: Growth and dieback of aspen forests in northwestern

619   Alberta, Canada, in relation to climate and insects, Canadian Journal of Forest Research, 32, 823-832,

620   2002.

621   Hogg, E., Brandt, J., and Michaelian, M.: Impacts of a regional drought on the productivity, dieback, and

622   biomass of western Canadian aspen forests, Canadian Journal of Forest Research, 38, 1373-1384, 2008.

623   Hogg, E. H.: Climate and the southern limit of the western Canadian boreal forest, Canadian Journal of

624   Forest Research, 24, 1835-1845, 1994.

625   Holdridge, L. R.: Determination of World Plant Formations From Simple Climatic Data, Science, 105, 367-

626   368, 10.1126/science.105.2727.367, 1947.

627   Hudiburg, T. W., Law, B. E., Wirth, C., and Luyssaert, S.: Regional carbon dioxide implications of forest

628   bioenergy production, Nature Climate Change, 1, 419-423, 10.1038/nclimate1264, 2011.

629   Hudiburg, T. W., Luyssaert, S., Thornton, P. E., and Law, B. E.: Interactive Effects of Environmental

630   Change and Management Strategies on Regional Forest Carbon Emissions, Environmental Science &

631   Technology, 47, 13132-13140, 2013.

632   Huxman, T. E., Smith, M. D., Fay, P. A., Knapp, A. K., Shaw, M. R., Loik, M. E., Smith, S. D., Tissue, D. T.,

633   Zak, J. C., and Weltzin, J. F.: Convergence across biomes to a common rain-use efficiency, Nature, 429,

634   651-654, 2004.

635   Jin, Y., and Goulden, M. L.: Ecological consequences of variation in precipitation: separating short-versus

636   long-term effects using satellite data, Global Ecology and Biogeography, 23, 358-370, 2014.

637   Johnstone, J. A., and Dawson, T. E.: Climatic context and ecological implications of summer fog decline in

638   the coast redwood region, Proceedings of the National Academy of Sciences, 107, 4533-4538, 2010.

639   Kang, S., Running, S. W., Kimball, J. S., Fagre, D. B., Michaelis, A., Peterson, D. L., Halofsky, J. E., and

640   Hong, S.: Effects of spatial and temporal climatic variability on terrestrial carbon and water fluxes in the

641   Pacific Northwest, USA, Environmental Modelling & Software, 51, 228-239, 2014.

642   Keith, H., Mackey, B. G., and Lindenmayer, D. B.: Re-evaluation of forest biomass carbon stocks and

643   lessons from the world's most carbon-dense forests, Proceedings of the National Academy of Sciences,

644   106, 11635-11640, 2009.

645   Kellndorfer, J., Walker, W., LaPoint, E., Bishop, J., Cormier, T., Fiske, G., Hoppus, M., Kirsch, K., and

646   Westfall, J.: NACP Aboveground Biomass and Carbon Baseline Data (NBCD 2000), U.S.A., 2000 Data set,

647   ORNL DAAC, Oak Ridge, Tennessee, U.S.A. , 2012.

648   Knapp, A. K., and Smith, M. D.: Variation among biomes in temporal dynamics of aboveground primary

649   production, Science, 291, 481-484, 2001.

650   Krankina, O. N., DellaSala, D. A., Leonard, J., and Yatskov, M.: High-Biomass Forests of the Pacific

651   Northwest: Who Manages Them and How Much is Protected?, Environmental Management, 54, 112-

652   121, 2014.

653   Law, B. E., Falge, E., Gu, L. V., Baldocchi, D. D., Bakwin, P., Berbigier, P., Davis, K., Dolman, A. J., Falk, M.,

654   and Fuentes, J. D.: Environmental controls over carbon dioxide and water vapor exchange of terrestrial

655   vegetation, Agricultural and Forest Meteorology, 113, 97-120, 2002.

656   Law, B. E., Sun, O. J., Campbell, J., Van Tuyl, S., and Thornton, P. E.: Changes in carbon storage and fluxes

657   in a chronosequence of ponderosa pine, Global Change Biology, 9, 510-524, 2003.

658   Lévesque, M., Siegwolf, R., Saurer, M., Eilmann, B., and Rigling, A.: Increased water-use efficiency does

659   not lead to enhanced tree growth under xeric and mesic conditions, New Phytologist, 203, 94-109, 2014.

660   Major, J.: A climatic index to vascular plant activity, Ecology, 44, 485-498, 1963.

661   McCabe, G. J., Palecki, M. A., and Betancourt, J. L.: Pacific and Atlantic Ocean influences on multidecadal

662   drought frequency in the United States, Proceedings of the National Academy of Sciences, 101, 4136-

663   4141, 2004.

664   McDowell, N. G., Williams, A., Xu, C., Pockman, W., Dickman, L., Sevanto, S., Pangle, R., Limousin, J.,

665   Plaut, J., and Mackay, D.: Multi-scale predictions of massive conifer mortality due to chronic

666   temperature rise, Nature Climate Change, 6, 295-300, 10.1038/nclimate2873, 2015.

667   Mitchell, K. E., Lohmann, D., Houser, P. R., Wood, E. F., Schaake, J. C., Robock, A., Cosgrove, B. A.,

668   Sheffield, J., Duan, Q., and Luo, L.: The multi-institution North American Land Data Assimilation System

669   (NLDAS): Utilizing multiple GCIP products and partners in a continental distributed hydrological

670   modeling system, Journal of Geophysical Research: Atmospheres, 109, 2004.

671   Mote, P. A., Snover, K., Capalbo, S., Eigenbrode, S. D., Glick, P., Littell, J., Raymondi, R., and Reeder, S.:

672   Northwest, in: Climate Change Impacts in the United States: The Third National Climate Assessment,

673   edited by: Melillo, J. M., Richmond, T. C. C., and Yohe, G. W., U.S. Global Change Research Program,

674   Washington, DC, 487-513, 2014.

Biogeosciences
Discussions

EGU
Open Access

675   Myneni, R., Hoffman, S., Knyazikhin, Y., Privette, J., Glassy, J., Tian, Y., Wang, Y., Song, X., Zhang, Y., and

676   Smith, G.: Global products of vegetation leaf area and fraction absorbed PAR from year one of MODIS

677   data, Remote sensing of environment, 83, 214-231, 2002.

678   Nakawatase, J. M., and Peterson, D. L.: Spatial variability in forest growth-climate relationships in the

679   Olympic Mountains, Washington, Canadian journal of forest research, 36, 77-91, 2006.

680   Olson, J. S.: Energy storage and the balance of producers and decomposers in ecological systems,

681   Ecology, 44, 322-331, 1963.

682   Pan, Y., Chen, J. M., Birdsey, R., McCullough, K., He, L., and Deng, F.: Age structure and disturbance

683   legacy of North American forests, 2011.

684   Peñuelas, J., Canadell, J. G., and Ogaya, R.: Increased water-use efficiency during the 20th century did

685   not translate into enhanced tree growth, Global Ecology and Biogeography, 20, 597-608, 2011.

686   Peterman, W., Waring, R. H., Seager, T., and Pollock, W. L.: Soil properties affect pinyon pine–juniper

687   response to drought, Ecohydrology, 6, 455-463, 2013.

688   R Core Team: R: A Language and Environment for Statistical Computing, R Foundation for Statistical

689   Computing, Vienna, 2015.

690   Ruefenacht, B., Finco, M., Nelson, M., Czaplewski, R., Helmer, E., Blackard, J., Holden, G., Lister, A.,

691   Salajanu, D., and Weyermann, D.: Conterminous US and Alaska forest type mapping using forest

692   inventory and analysis data, Photogramm. Eng. Remote Sens, 74, 1379-1388, 2008.

693   Ruehr, N., Law, B., Quandt, D., and Williams, M.: Effects of heat and drought on carbon and water

694   dynamics in a regenerating semi-arid pine forest: a combined experimental and modeling approach,

695   Biogeosciences, 11, 4139-4156, 2014.

696   Running, S. W.: Testing Forest-BGC Ecosystem Process Simulations Across a Climatic Gradient in Oregon,

697   Ecological Applications, 4, 238-247, 1994.

698   Running, S. W., Nemani, R. R., Heinsch, F. A., Zhao, M., Reeves, M., and Hashimoto, H.: A continuous

699   satellite-derived measure of global terrestrial primary production, BioScience, 54, 547-560, 2004.

700   Runyon, J., Waring, R., Goward, S., and Welles, J.: Environmental limits on net primary production and

701   light-use efficiency across the Oregon transect, Ecological Applications, 4, 226-237, 1994.

702   Sanford, W. E., and Selnick, D. L.: Estimation of Evapotranspiration Across the Conterminous United

703   States Using a Regression With Climate and Land-Cover Data1, JAWRA Journal of the American Water

704   Resources Association, 49, 217-230, 2013.

705   Schroeder, P. E., McCandlish, B., Waring, R. H., and Perry, D. A.: The relationship of maximum canopy

706   leaf area to forest growth in eastern Washington, Northwest Science, 56, 121-130, 1982.

707   Schuur, E. A.: Productivity and global climate revisited: the sensitivity of tropical forest growth to

708   precipitation, Ecology, 84, 1165-1170, 2003.

709   Schwalm, C. R., Williams, C. A., Schaefer, K., Baldocchi, D., Black, T. A., Goldstein, A. H., Law, B. E.,

710   Oechel, W. C., and Scott, R. L.: Reduction in carbon uptake during turn of the century drought in western

711   North America, Nature Geoscience, 5, 551-556, 2012.

712   Seager, R., and Vecchi, G. A.: Greenhouse warming and the 21st century hydroclimate of southwestern

713   North America, Proceedings of the National Academy of Sciences, 107, 21277-21282, 2010.

714   Singh, D., Swain, D. L., Mankin, J. S., Horton, D. E., Thomas, L. N., Rajaratnam, B., and Diffenbaugh, N. S.:

715   Recent amplification of the North American winter temperature dipole, Journal of Geophysical

716   Research: Atmospheres, 2016.

717   Smith, J. E., Heath, L. S., Skog, K. E., and Birdsey, R. A.: Methods for calculating forest ecosystem and

718   harvested carbon with standard estimates for forest types of the United States, USDA Forest Service

719   General Technical Report NE-343, Newtown Square, PA, 222, 2006.

720   Soulé, P. T., and Knapp, P. A.: Analyses of intrinsic water-use efficiency indicate performance differences

721   of ponderosa pine and Douglas-fir in response to CO_2 enrichment, Journal of Biogeography, 42, 144-

722   155, 2015.

723   Spies, T. A., Ripple, W. J., and Bradshaw, G.: Dynamics and pattern of a managed coniferous forest

724   landscape in Oregon, Ecological Applications, 4, 555-568, 1994.

725   Thomas, C. K., Law, B. E., Irvine, J., Martin, J. G., Pettijohn, J. C., and Davis, K. J.: Seasonal hydrology

726   explains interannual and seasonal variation in carbon and water exchange in a semiarid mature

727   ponderosa pine forest in central Oregon, Journal of Geophysical Research: Biogeosciences (2005–2012),

728   114, 2009.

729   Van Tuyl, S., Law, B., Turner, D., and Gitelman, A.: Variability in net primary production and carbon

730   storage in biomass across Oregon forests—an assessment integrating data from forest inventories,

731   intensive sites, and remote sensing, Forest Ecology and Management, 209, 273-291, 2005.

732   Walsh, J., Wuebbles, D., Hayhoe, K., Kossin, J., Kunkel, K., Stephens, G., Thorne, P., Vose, R., Wehner, M.,

733   Willis, J., Anderson, D., Doney, S., Feely, R., Hennon, P., Kharin, V., Knutson, T., Landerer, F., Lenton, T.,

734   Kennedy, J., and Somerville, R.: Our Changing Climate, in: Climate Change Impacts in the United States:

735   The Third National Climate Assessment, edited by: Melillo, J. M., Richmond, T. C., and Yohe, G. W., U.S.

736   Global Change Research Program, 19-67, 2014.

737   Waring, R.: Estimating forest growth and efficiency in relation to canopy leaf area, Adv. Ecol. Res, 13,

738   327-354, 1983.

739   Waring, R. H., and Franklin, J. F.: Evergreen coniferous forests of the Pacific Northwest, Science, 204,

740   1380-1386, 1979.

741   Waring, R. H., and Running, S. W.: Forest Ecosystems: Analysis at Multiple Scales, 3rd ed., Elsevier

742   Academic Press, Burlington, MA, 420 pp., 2007.

743   Webb, W. L., Lauenroth, W. K., Szarek, S. R., and Kinerson, R. S.: Primary production and abiotic controls

744   in forests, grasslands, and desert ecosystems in the United States, Ecology, 134-151, 1983.

745   Whittaker, R. H., and Niering, W. A.: Vegetation of the Santa Catalina Mountains, Arizona. V. Biomass,

746   production, and diversity along the elevation gradient, Ecology, 56, 771-790, 1975.

747   Wickham, H., and Francois, R.: dplyr: A Grammar of Data Manipulation, R package version 0.4.2,

748   http://CRAN.R-project.org/package=dplyr, 2015.

749   Williams, A. P., Allen, C. D., Macalady, A. K., Griffin, D., Woodhouse, C. A., Meko, D. M., Swetnam, T. W.,

750   Rauscher, S. A., Seager, R., and Grissino-Mayer, H. D.: Temperature as a potent driver of regional forest

751   drought stress and tree mortality, Nature Climate Change, 3, 292-297, 2012.

752   Williams, A. P., Seager, R., Macalady, A. K., Berkelhammer, M., Crimmins, M. A., Swetnam, T. W.,

753   Trugman, A. T., Buenning, N., Noone, D., and McDowell, N. G.: Correlations between components of the

754   water balance and burned area reveal new insights for predicting forest fire area in the southwest

755   United States, International Journal of Wildland Fire, 24, 14-26, 10.1071/WF14023, 2014.

756   Williams, M., Rastetter, E., Fernandes, D., Goulden, M., Wofsy, S., Shaver, G., Melillo, J., Munger, J., Fan,

757   S. M., and Nadelhoffer, K.: Modelling the soil-plant-atmosphere continuum in a Quercus–Acer stand at

758   Harvard Forest: the regulation of stomatal conductance by light, nitrogen and soil/plant hydraulic

759   properties, Plant, Cell & Environment, 19, 911-927, 1996.

760   Williams, M.: Deforesting the Earth: From Prehistory to Global Crisis, University of Chicago Press,

761   Chicago, USA, 543 pp., 2006.

762   Wilson, B. T., Woodall, C., and Griffith, D.: Imputing forest carbon stock estimates from inventory plots

763   to a nationally continuous coverage, Carbon balance and management, 8, 1, 2013.

764   Yang, Y., Fang, J., Ma, W., and Wang, W.: Relationship between variability in aboveground net primary

765   production and precipitation in global grasslands, Geophysical Research Letters, 35, 2008.

766   Zhao, M., Running, S., Heinsch, F. A., and Nemani, R.: MODIS-derived terrestrial primary production, in:

767   Land Remote Sensing and Global Environmental Change: NASA's Earth Observing System and the

768   Science of ASTER and MODIS, edited by: Ramachandra, B., Justice, C. O., and Abrams, M. J., Springer,

769   New York, 635-660, 2010.

770   Zotarelli, L., Dukes, M. D., Romero, C. C., Migliaccio, K. W., and Morgan, K. T.: Step by step calculation of

771   the Penman-Monteith Evapotranspiration (FAO-56 Method), Institute of Food and Agricultural Sciences.

772   University of Florida, 2010.

773

774

775

776

777

778

779

780

781

782

783

784

785

786

787

788

789 **Tables**

790 **Table 1.** Summary of tree net primary productivity (NPP; Mg C ha^{-1} yr^{-1}), live biomass (BIO; Mg C ha^{-1}),

791 and carbon residence time (CRT; year) for stands over 100 years old across both WAORCA and the

792 broader western US. These forest characteristics were quantified for WAORCA using field measurements

793 from 1,953 sites and for the western US using satellite-derived data sets covering 18 Mha of mature

794 forest. Satellite data sets included MODIS NPP and an estimate of BIO derived by combining existing

795 maps of aboveground biomass with additional estimates of carbon storage in coarse root, fine roots, and

796 foliage. CRT describes the average duration, in years, that a molecule of carbon will remain in live tree

797 biomass and was computed as CRT=BIO/NPP. It is also known as the biomass accumulation ratio. These

798 carbon stocks and fluxes combine above- and below-ground components.

Domain	Variable	Units	Time span	Mean (SD)	Range
WAORCA	NPP_{field}	Mg C ha^{-1} yr^{-1}	2001-2006	4.3 (2.5)	0.6 – 20.9
	BIO_{field}	Mg C ha^{-1}	2001-2006	158 (135)	2 – 947
	CRT_{field}	year	2001-2006	33 (19)	2 – 137
Western US	NPP_{sat}	Mg C ha^{-1} yr^{-1}	2000-2014	5.3 (2.0)	0.1 – 227
	BIO_{sat}	Mg C ha^{-1}	2000-2008	83 (54)	2 – 669
	CRT_{sat}	year	2000-2008	15 (9)	2 – 1390

799

800

801

802

803

804

805

806

807

808

809

Biogeosciences
Discussions

Open Access

EGU

810 **Table 2.** Changes in tree net primary productivity (NPP; Mg C ha^{-1} yr^{-1}), live biomass (BIO; Mg

811 C ha^{-1}), and carbon residence time (CRT; year) for stands over 100 years old along gradients in a

812 climate moisture index (CMI$_{\overline{wy}}$; cm yr^{-1}) in both WAORCA and the broader western US. Forest

813 characteristics were quantified using field measurements in WAORCA and satellite remote

814 sensing data sets covering the western US. The analysis incorporated forests in areas where

815 CMI$_{\overline{wy}}$ was between -200 cm yr^{-1} and 200 cm yr^{-1}. Summaries include (1) median forest

816 characteristic in the driest 5% and wettest 95% of sites/pixels; (2) the corresponding change; (3)

817 and the Spearman correlation (r_s) between CMI$_{\overline{wy}}$ and the median forest characteristic computed

818 at 10 cm yr^{-1} CMI$_{\overline{wy}}$ intervals. All correlations were statistically significant at $\alpha < 0.001$.

Domain	Variable	Units	Median of…		Change…		CMI$_{\overline{wy}}$ cor.
			Driest 5%	Wettest 95%	Abs.	%	r_s
WAORCA	NPP$_{field}$	Mg C ha^{-1} yr^{-1}	2.2	5.6	3.4	155	0.93
	BIO$_{field}$	Mg C ha^{-1}	26	281	255	997	0.96
	CRT$_{field}$	year	11	49	38	358	0.96
Western US	NPP$_{sat}$	Mg C ha^{-1} yr^{-1}	3.4	6.7	3.3	97	0.93
	BIO$_{sat}$	Mg C ha^{-1}	32	165	133	410	0.97
	CRT$_{sat}$	year	10	26	16	160	0.99

819

820

821

822

823

824

825

826

827

828
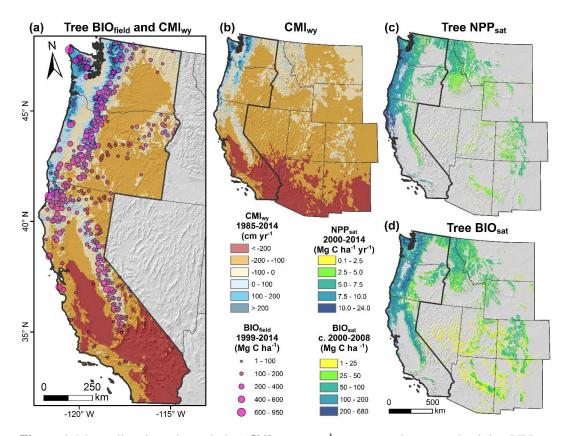
829

830

831

Figure 1. Mean climatic moisture index (CMI$_{\overline{wy}}$; cm yr^{-1}), tree net primary productivity (NPP; Mg C ha^{-1} yr^{-1}), and live tree biomass (BIO; Mg C ha^{-1}) in the western US. (a) BIO derived from field measurements (BIO$_{field}$) at mature sites (>100 years) in WAORCA. For visual clarity only 20% of the 1,953 sites are depicted. (b) CMI$_{\overline{wy}}$ was computed as monthly precipitation minus reference evapotranspiration summed over the annual water year (October-September) and then averaged from 1985-2014. (c) Mean annual NPP was quantified using MODIS satellite data from 2000-2014 (NPP$_{sat}$). (d) BIO was quantified using satellite-derived estimates of carbon stocks (BIO$_{sat}$).
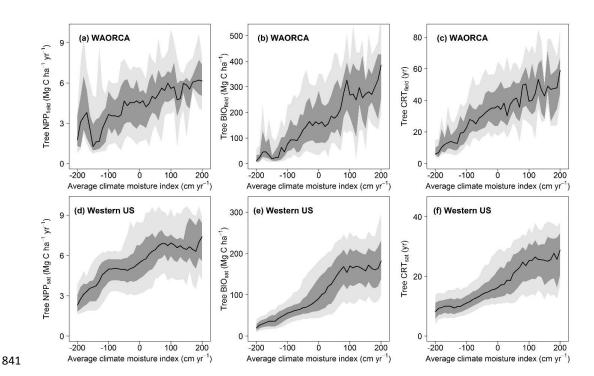
840

Figure 2. Tree net primary productivity (NPP; Mg C ha^{-1} yr^{-1}), live biomass (BIO; Mg C ha^{-1}),

and carbon residence time (CRT; years) increased with increasing climatic water availability

across both WAORCA (a-c) and the broader western US (d-f). Forest characteristics were

derived from field measurements on 1,953 inventory plots in WAORCA (a-c) and from satellite

remote sensing data sets across 18 Mha of mature forest in the western US (d-f). NPP$_{sat}$ was

characterized using MODIS data averaged annual from 2000 to 2014. BIO$_{sat}$ was quantified

based on an ensemble of aboveground biomass maps plus estimates of coarse root, fine root, and

foliage biomass. CRT was computed for each field plot and pixel as BIO / NPP. Water

availability was quantified using a climate moisture index (CMI= P-ET$_0$) summed over the water

year (October-September) and then averaged from 1985-2014 (CMI$_{\overline{wy}}$). The region was

partitioned into 10 cm yr^{-1} (non-overlapping) CMI$_{\overline{wy}}$ bins, pixels/plots were allocated to bins,

and then forest characteristics were summarized within each bin. In each panel, the bold line

854   denotes the median, dark gray band the 25-75th percentiles, and light gray band the 10-90th

855   percentiles. Note the different y-axis scales between (b) and (e), as well as (c) and (f).

856